

# Human optic sensitivity computation based on singular value decomposition

SEYED ALI AMIRSHAH<sup>1</sup>, FARAH TORKAMANI-AZAR<sup>2\*</sup>

<sup>1</sup>Chair of Computer Vision, Friedrich Schiller University, Jena, Germany

<sup>2</sup>Cognitive Telecommunication Research Group, Faculty of Electrical and Computer Engineering,  
Shahid Beheshti University, G.C., Tehran, Iran

\*Corresponding author: f-torkamani@sbu.ac.ir

In this paper, a new definition for images named as the sensitivity parameter (SP) is introduced. SP is based on the decreasing rate of singular values in an image. It could be used in compressing images in a lower bit rate or in distinguishing robust image parts against watermarking. SP could also be used when we would want to make changes in pixel values but keep the quality of the image as it is.

Keywords: image processing, image complexity, singular value decomposition, sensitivity parameter.

## 1. Introduction

The aim of this paper is to present a new parameter named as the sensitivity parameter (SP). SP is only based on information obtained from human evaluation to locally determine the amount of complexity or spatial activity in an image structure. Based on human evaluation, even if different structure parts have the same frequency or same brightness they do not seem equal. This is because human observers are not able to equally focus on image details. An important factor of SP is its ability to separate pixels with respect to their structural and sensitivity of observation. For this reason, SP could be used in applications such as finding the best bit rate in compression without decreasing the image quality, finding the most suitable part to embed watermarks, determining the most important parts to enhance in noisy images, etc. Some research is reported to be done on image complexity using statistical information such as entropy, variance, edge position and other statistical methods [1–3]. Also, in video coding, the spatial activity of macro blocks should be detected. These blocks would be more robust against intra-prediction models. A drawback of statistical methods is that they treat pixel values individually without considering their situation and the neighboring pixels. Another approach taken consists in using the fuzzy theory to

distinguish image complexity in three classes [4]. In this study, we propose a new approach to face this issue. The proposed method is based on singular value decomposition (SVD) theorem. The SVD is a method for identifying and ordering the dimension along the data points which exhibit the greatest variation. SVD is based on a theorem from linear algebra which says that a rectangular matrix  $A$  can be broken down into the product of three matrices, an orthogonal matrix  $U$ , a diagonal matrix  $\Lambda$ , and the transpose of an orthogonal matrix  $V$ . The theorem is usually presented as follows:

$$A_{m \times n} = U_{m \times m} \cdot \Lambda_{m \times n} \cdot V_{n \times n}^T \quad (1)$$

where  $U^T U = I$  and  $V^T V = I$ ; ( $I$  is the identity matrix). The columns of  $U = \{U_1, U_2, \dots, U_m\}$  are orthonormal eigenvectors of  $AA^T$ , the columns of  $V = \{V_1, V_2, \dots, V_n\}$  are orthonormal eigenvectors of  $A^T A$ , and  $\Lambda$  is a diagonal matrix containing singular values,  $\lambda_i$ , in descending order. If we consider  $m < n$ , only  $m$  nonzero singular values are computed and indicate the vector  $\Gamma = \{\lambda_i\}_{i=1}^m$ . In fact, SVD uses statistical properties while considering their distribution as well.

In Section 2, the proposed approach is introduced, Section 3 is dedicated to the experimental results and a conclusion of the work is given in Section 4.

## 2. Approach proposed

It should be noted that the mean value and standard deviation (SD) in each matrix are not related to how pixels are set in the block. Consider the three blocks in Fig. 1 which have the same pixel values in different distributions. Although their variance and mean

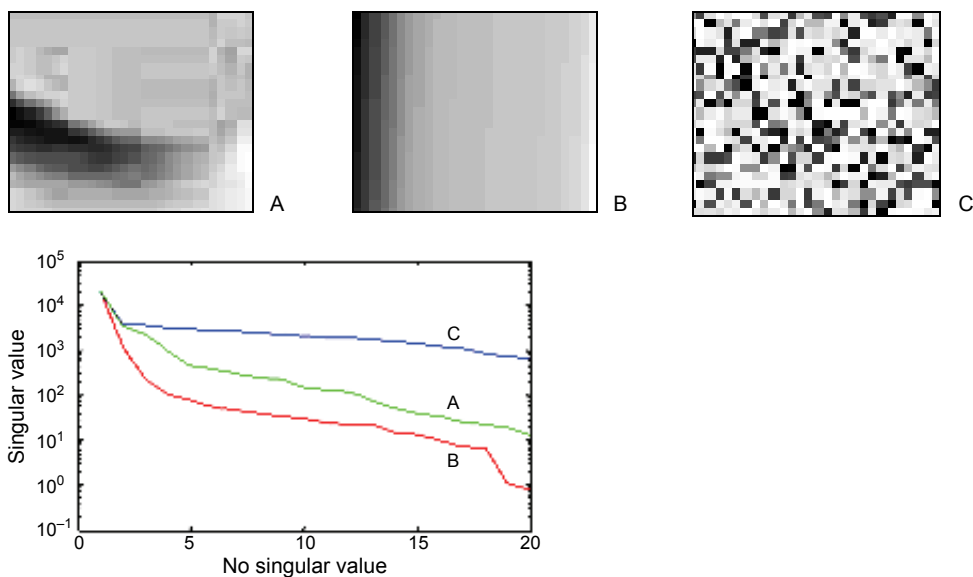


Fig. 1. Three blocks with the same histogram and different distributions and a plot of their singular values.

Table 1. The statistical parameters of the blocks shown in Fig. 1.

Block	Mean of blocks	SD of blocks	$s_2/s_1$	$s_3/s_1$	$s_4/s_1$
A	55.87	8.5	0.16	0.11	0.050
B	55.87	8.5	0.05	0.01	0.005
C	55.87	8.5	0.18	0.17	0.150

values are equal, but as seen in Fig. 1 their singular values are completely different. This is due to the fact of the different frequency definition being embedded in the SVD theorem. The first singular values show the effects of low frequency components which are effective in constructing the structure of image and the last ones define the high frequency components which have an effect on constructing the details in the image. In other words, in complex areas, all singular values are important and we would have approximately a uniform distribution. Table 1 shows the ratio of second, third and fourth singular values to the first one for the three blocks shown in Fig. 1.

According to Weber's ratio, the ability of the eye to discriminate between changes in light intensity is related to background brightness. So, when the value of brightness area is high, to distinguish objects, a large percentage change in intensity is required. However, in dark areas, a small percentage in intensity could be enough [5]. Therefore, we would face a decrease in the quality of a redundant object when a brightness with large difference value from the background's intensity is inserted in bright areas of the image. This happens in dark areas with a small difference value in brightness. This is why considering the mean value of the block is necessary to distinguish bright areas as well. In addition, consider the blocks shown in Fig. 1, the change of a pixel value in block C is not recognized, it is also not important for the observer as it is in other blocks. For this reason, image complexity or sensitivity to value changes after watermarking or denoising should be considered differently in different blocks. This information could also be used in the case of block compression. If we need to increase SNR, the blocks like block C could be compressed with high bit rate. However, in the case of increasing requirement of quality, or storing bit rate, the blocks like block C could be compressed with a fewer bit rate, although its reconstruction error would be large, it would not be detectable for observers. To compute sensitivity we have to consider all parameters. As a result, the bright areas with a low decreasing rate in singular values would have less sensitivity to brightness mutation. For this reason we will give each pixel of the original image,  $f$ , a value of sensitivity as follows:

1. Consider a sliding block with a size of  $n \times n$  (odd  $n$ ) surrounding the pixel  $(i, j)$  which is denoted  $w_{ij}$ . However, we consider  $i$  and  $j$  as (for an  $M \times N$  image):

$$\frac{n+1}{2} \leq i \leq M - \frac{n-1}{2}$$

$$\frac{n+1}{2} \leq j \leq N - \frac{n-1}{2}$$

Since  $n \ll M$  and also  $n \ll N$ , this be to convenient and not affect the procedure results.

2. Compute singular values of each block  $w_{ij}$  as  $\Gamma_{ij} = \{\lambda_\gamma\}_{\gamma=1}^n$  via the singular value theorem.

3. Compute the decreasing rate as:

$$k_1(i, j) = \left[ \frac{\lambda_3}{\lambda_1} + \frac{\lambda_4}{\lambda_1} \right] \quad (2)$$

Since, in all different image structures, the rate of the second singular value to the first one has a large value, we decided to consider the decreasing rate as Eq. (2). However, the ratio of the reminder singular values is the same. Because of decreasing complexity in computation, we restricted ourselves to this equation only.

4. Compute the ratio of mean brightness value of block  $w_{ij}$  as  $\mu(i, j)$  with respect to the mean pixel brightness of the original image  $f$ .

$$k_2(i, j) = \frac{\mu(i, j)}{f} \quad (3)$$

5. Compute the effects of brightness value and singular values decreasing rate:

$$a(i, j) = k_1(i, j)k_2(i, j) \quad (4)$$

6. Compute the following equation as a sensitivity parameter that is limited between zero and one:

$$\text{SP}(i, j) = 1 - \frac{a(i, j)}{\max_{i,j}\{a(i, j)\}} \quad (5)$$

In Equation (4), we recognize the areas which are bright and also have a decreasing pattern in the first singular values. In the final step, parameter  $a(i, j)$  should be normalized to the maximum values of  $a$ 's. Equation (5) is bounded by zero for the least sensitive area and one for the most sensitive area. Our aim is to recognize the irregular chaotic areas as the less sensitive ones. In this case, to have the observable brightness change, it is necessary to change the brightness of pixels with large values. So, the area with a less sensitive value could be compressed with a low bit rate.

### 3. Experimental results

In the first step, we calculate the sensitivity values of all the pixels for three different images from the LIVE database [6, 7]. The images are selected at different complexity levels and different types of smooth areas and edges. Although the size of the sliding block could be different, it seems that if  $n$  is considered as 3, each pixel is compared only with its nearest neighboring pixels. On the other hand, if we consider  $n$  as a large value, it could be confused for small objects. To observe different situations 3 different values of  $n$  ( $n = 3, 5$  and  $7$ ) were tested on all images. It was seen that  $n = 5$  could be a suitable value for all images with different levels of complexity. Their sensitivity



Fig. 2. First row: original images, second row: sensitivity maps, third row: binary images of the second row used with a threshold level of 0.5.

maps are computed using a window of the size of  $5 \times 5$ . Figure 2 shows three original images from the LIVE database and their sensitivity maps. In addition, as an example binary maps of the sensitivity map using a threshold level of 0.5 are shown in the third row.

As seen in Fig. 2, the areas which are covered by the plants (seen in the bottom corners of the *Building 2* image) are identified as a less sensitive area; note that they have different brightness values. In the case of the *Caps* image, we are facing an image with a low complexity which contains large smooth areas (hence few changes in pixel values could be observable). As can be seen, sensitivity values are large in textured areas, and small in the spaces between the caps on the board.

To use this idea in image compression, we first simulated a test image of ocean. As seen in the binary image of the sensitivity map of ocean in Fig. 2, the top half part of the image (part 1) has approximately a sensitivity value larger than 0.5, while the sensitivity value of the bottom part (part 2) is smaller than 0.5. We partitioned this image in two equal parts and compressed each part with a bit rate different from the other part. Compressions are done using the jpeg compression command in MATLAB as seen in Tab. 2. These images after reconstruction are shown in Fig. 3.

Table 2. SNR of *Ocean* image using different compression quality degrees.

	Part 2		
	75%	50%	25%
Part 1	39.66 dB	37.92 dB	36.39 dB
	39.98 dB	37.45 dB	36.06 dB
	38.15 dB	36.85 dB	35.61 dB

Fig. 3. *Ocean* image with different quality jpeg compression degrees: part 1 – 75%, part 2 – 75% (a), part 1 – 75%, part 2 – 25% (b), part 1 – 25%, part 2 – 75% (c).

As seen, however, images have been compressed at different bit rates, after reconstruction, their appearances look fine. As can be seen in Tab. 2, if we compress parts of the image that are less sensitive with a higher compression rate, we will still have an image with the same quality. This is due to the complexity of the region distortions being invisible. On the other hand, these changes decrease the SNR significantly; SNR is computed for reconstructed image as  $g$  and original image as  $f$ :

$10 \log \left\{ \sum_{m, n} [f(m, n)]^2 / \sum_{m, n} [f(m, n) - g(m, n)]^2 \right\}$ . This is why changing the bit rate in the lower region which is also the region with a lower sensitivity would have an effect on the SNR. The first row of Tab. 2 shows the change in bit rates for the region with lower sensitivity.

To generalize the idea of image compression, we decided to use all reference images in the LIVE database. We will first divide the images in parts of  $32 \times 32$  pixels. In the next step, we will compute the mean sensitivity of each segment and use different quality jpeg compression degrees for compressing each segment as follows:

- If the mean sensitivity values of block are smaller than 0.25; jpeg quality degree is set to 25%;
- If the mean sensitivity values of block are between 0.25 and 0.5; jpeg quality degree is fixed to 50%;
- If the mean sensitivity values of block are larger than 0.5; jpeg quality degree is set to 75%.

Since, in this case, we used the mean of sensitivity parameters, removing the effect of the border pixels, which was discussed in step a of the algorithm in the previous section, would not be lead to any important error.

Table 3. Results of 29 images of LIVE database and three measured parameters.

Name	$P_1$	$P_2$	$P_3$	Name	$P_1$	$P_2$	$P_3$
Bikes	3.3333	5.4688	0.0248	Ocean	7.6923	17.7083	0.0409
Building 2	5.102	9.6875	0.0268	Painted	8.2192	16.6667	0.0347
Buildings	4.3011	5.2083	0.0210	Parrots	8.8235	8.0729	0.0158
Caps	12.5	18.2292	0.0332	Plane	12.5	9.6354	0.0275
Carnivaldolls	10.869	23.1579	0.0361	Rapids	5.3333	11.7188	0.0351
Cemetery	7.9365	23.5088	0.0409	Sailing 1	7.3529	20.3125	0.0409
Churchand	9.2593	29.8246	0.0427	Sailing 2	10.8108	16.9697	0.0248
Coinsinfout	7.8125	13.4375	0.0328	Sailing 3	9.5238	11.2121	0.0233
Dancers	4.918	13.1579	0.0296	Sailing 4	9.6774	16.6667	0.0434
Flowerson	9.5238	31.5625	0.0425	Statue	10.8696	19.0909	0.0348
House	8.4746	16.6667	0.0401	Stream	9.434	21.0938	0.0582
Lighthouse	11.5385	27.8788	0.0472	Students	6.4935	20.7018	0.0308
Lighthouse 2	10.1695	25.5208	0.0350	Woman	7.8125	15.4545	0.0356
Manfishing	2.2727	2.4291	0.0175	Womanhat	6.8182	8.787	0.0268
Monarch	6.5217	13.2813	0.0144	Average	8.1343	16.3142	0.033

The images with different jpeg quality degrees after reconstruction are denoted by  $g$ . In addition, the whole image was compressed with a jpeg quality degree of 75% and was denoted as  $f$ .

To evaluate the effect of the proposed sensitivity idea, three parameters were calculated (see Tab. 3) as follows:

- The percentage of the reduction in storage memory:

$$P_1 = \frac{\text{requirement storage of } g}{\text{requirement storage of } f} \times 100\% \quad (6)$$

- The percentage of low sensitivity areas to the whole image:

$$P_2 = \frac{N_{0.25}}{N} \times 100\% \quad (7)$$

where  $N_{0.25}$  and  $N$  are the number of blocks with a mean of sensitivity parameter smaller than 0.25 and the number of all blocks, sequentially,

$$P_3 = \text{SSIM}_f - \text{SSIM}_g \quad (8)$$

where  $\text{SSIM}_f$  and  $\text{SSIM}_g$  are the structural similarity index (SSIM) for  $f$  and  $g$  images, respectively. In other words, SSIM is the quality value of  $f$  and  $g$ , respectively [8].

As seen in Tab. 3, using the sensitivity idea would lead us to a decrease in the compression bit rate by 8% on average, while the observation quality is simultaneously preserved. In addition, the maximum and minimum difference of  $P_2$  belongs to *Flowerson* and *Manfishing*. The results of applying two compression

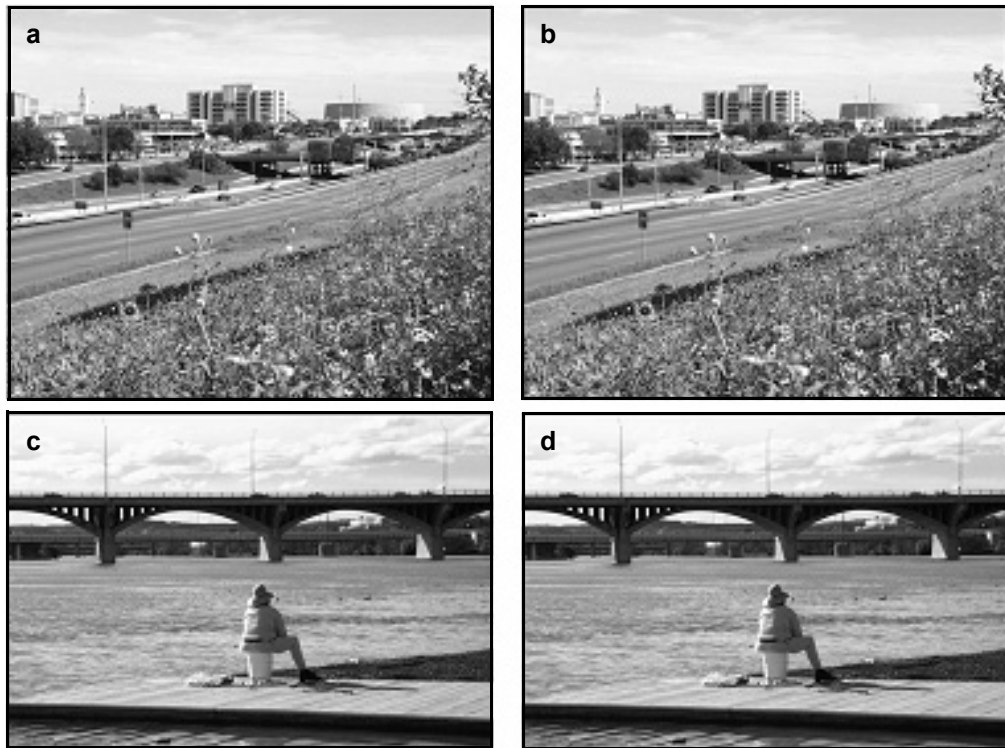


Fig. 4. Reconstructed images *Flawerson* and *Manfishing* after: compression with different quality degrees SSIM = 0.9273 (**a**), compression with one quality degree, SSIM = 0.9698 (**b**), compression with different quality degrees SSIM = 0.9442 (**c**), compression with one quality degree, SSIM = 0.9617 (**d**).

methods in the two images are shown in Fig. 4. As seen in the case of the *Flawerson* image, using different jpeg compression rates leads to a decrease in the bit rate of up to 9.5%, while the SSIM quality value has a reduction of only 0.04 and observers are not able to distinguish this difference.

To see the SP effect in image quality, we consider the two images shown in Fig. 4, in five cases of different distortion in the LIVE database. Table 4 shows the comparison results. In each distortion type, we consider the lowest and highest distorted images and the difference of their quality degrees from the LIVE database which has been called the difference mean opinion score (DMOS) value.

As seen in Table 4, the decreasing rate of quality in the case of *Flawerson* which has a larger  $P_2$  in comparison to the *Manfishing* image is smaller, except in the case of blurring. Other distortions caused a small decrease in the quality rate when small bit rates were used in compressing the *Flawerson* image. In the case of regions which have a low SP, since these areas have high frequencies, the blurring affects the observer's estimation of the quality. On the other hand, in regions with high

Table 4. The decreasing rate of DMOS values for the five types of the lowest and the highest distortion.

Distortion type	Image	
	Flowerson	Manfishing
Additive noise	46	50
Gaussian blur	44.4	37.5
Fast fading	22.1	30
Jpeg compression	34.5	50.1
JP2k compression	45	48

sensitivity, we will have uniform regions in which blurring would not have a huge effect on the quality of the region. In summary, images with large  $P_2$  are more robust with respect to noise and compression compared to images with small  $P_2$  values.

## 4. Conclusions

In this paper, we introduced a new parameter which helps compute the sensitivity of images with respect to the changes in pixel values. The parameter can be used when watermarking an image and/or using different bit rates to compress an image. This parameter considers the rate of decreasing singular values in masks surrounding the pixel. In smooth areas, the second and third singular values fall too abruptly. In the case of a high spatial activity, the second and third singular values are large compared to the first singular value and so could play an effective role in the image structure. The idea is supported by some practical applications and the experiments show that the sensitivity parameter could be used to control the required bit rate to compress images. Experiments have shown that by using different quality jpeg compression in the non-overlapping parts of an image, we could save a storage memory of up to 12.5%.

## References

- [1] QUAN PANG, CUIRONG YANG, YINGLE FAN, PING XU, *Texture image segmentation based on description complexity*, IEEE International Conference on Control and Automation, Gaungzhou, China, 2007, pp. 2848–2850.
- [2] LEMPEL A., ZIV J., *On the complexity of finite sequences*, IEEE Transactions on Information Theory **22**(1), 1976, pp. 75–81.
- [3] ZHANG P., ZHAO S., PENG S., *A texton-based algorithm of texture image segmentation*, Journal of Image and Graphics **8**, 2003, pp. 896–901.
- [4] BANERJEE S., MUKHERJEE D.P., DUTTA MAJUMDAR D., *Fuzzy c-means approach to tissue classification in multimodal medical imaging*, Information Sciences **115**(1–4), 1991, pp. 261–279.
- [5] GONZALEZ R.C., WOODS R.E., *Digital Image Processing*, Prentice-Hall, NJ, 2nd Edition, 2002.
- [6] SHEIKH H.R., WANG Z., CORMACK L., BOVIK A.C., *Live Image Quality Assessment Database, Release 2005*, <http://live.ece.utexas.edu/research/quality>.

- [7] SHEIKH H.R., BOVIK A.C., DE VECIANA G., *An information fidelity criterion for image quality assessment using natural scene statistics*, IEEE Transactions on Image Processing **14**(12), 2005, pp. 2117–2128.
- [8] ZHOU WANG, BOVIK A.C., *A universal image quality index*, IEEE Signal Processing Letters **9**(3), 2002, pp. 81–84.

*Received March 3, 2011  
in revised form September 13, 2011*